ECF22 - Loading and Environmental effects on Structural Integrity

Study of the dynamic fracture of hollow spheres under compression using the Discrete Element Method

A. Coré[a], J.-B. Kopp[a,*], J. Girardot[a,*], P. Viot[a]

[a]*Arts et Métiers ParisTech, CNRS, I2M Bordeaux, Esplanade des Arts et Métiers, Talence 33400, France*

Abstract

Hollow sphere structure (HSS) belongs to cellular solids that have been studied recently for its multiples properties. In our case, HSS aims to absorb soft impacts energy on an airliner cockpit. This structure is investigated because of its promises in term of specific energy dissipated (J.kg1) during impact. First of all, quasi- static and dynamic ($v = 5\,mm\,min^{-1}$ to $v = 2\,m\,s^{-1}$) uniaxial compression tests are conducted at room temperature on a single sphere (D = 30 mm). Rapid crack propagation (RCP) is observed to be predominant at macroscopic scale. The formalism of Linear Elastic Fracture Mechanics (L.E.F.M.) is therefore used to estimate the dynamic energy release rate G_{Idc} . The crack tip location is measured during the crack propagation using a high speed camera. The Discrete Element Method (DEM) is used to simulate the dynamic fracture by implementing a node release technique to perform a generation phase simulation. The dynamic energy release rate can be determined using the experimentally measured crack history. In hollowed spherical structures the numerical results reveal a high proportion of energy dissipated through inertial effects as well as a dependence of the thickness of the skin over the range of 0.04 mm to 1.2 mm. At a crack tip velocity of 0.6 times the Rayleigh wave speed of the material, the dynamic correction factor is less than 0.05. Similar results have been shown for the longitudinal dynamic fracture of polymer pipes. The quantitative results of GIdc are in good agreement with the literature and the present model offers an alternative to the finite element method to simulate the rapid crack propagation.Its use reveals to be an interesting way to model the mechanical behavior of brittle materials.

Keywords: Dynamic fracture; Discrete Element Method; Impact; Hollow spheres

1. Introduction

Hollow sphere structure (HSS) belongs to cellular solids that have been studied recently for their multiple properties (Augustin, 2009). Compared to foam structure, HSS has both closed and open porosity. Its applications can be of various types including energy absorber (Rahmé et al., 2012), acoustic damping (Gasser et al., 2003), and thermal insulation (Fiedler et al., 2008). In our case, HSS aims to absorb soft impacts energy on an airliner cockpit. Most of impacts are due to bird-strikes during take-off or landing at high velocity (maximum velocity is about $175\,m\,s^{-1}$).

* Corresponding authors : J.-B. Kopp & J. Girardot
E-mail address: jean-benoit.kopp@ensam.eu & jeremie.girardot@ensam.eu

10.1016/j.prostr.2018.12.288

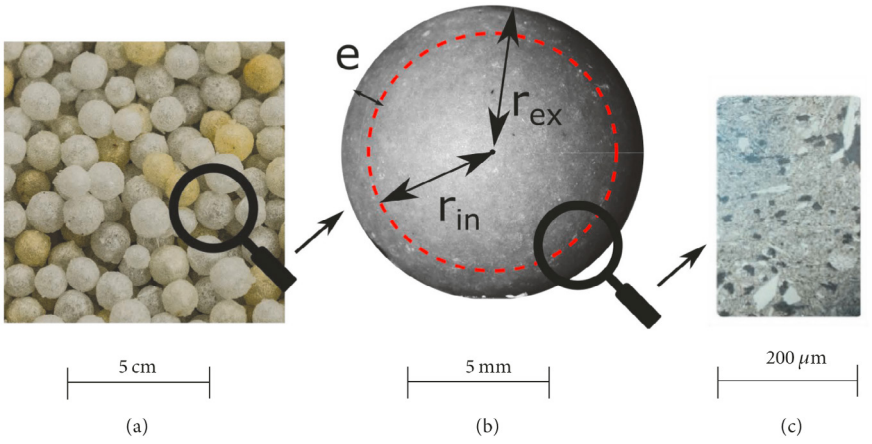

Fig. 1. Hollow sphere structure (a), hollow spheres parameters (b), and an optical microscope capture of the constitutive material (c).

Hollow spheres used in this study are made of commercial epoxy resin, a thermosetting polymer subjected to crack propagation (Kausch, 2012). A rapid crack propagation (RCP) is observed, and reveals to be predominant at macroscopic scale to dissipate the available energy stored in the structure (Yamini and Young, 1980).

The dynamic fracture of the constitutive material in HSS needs to be studied. The first part of this work was to evaluate the compressive behavior of on HSS related to a static and a dynamic loading. The force-displacement results allow to get the dissipated energy during the compression. In the second part of the paper, a numerical analysis was performed in order to quantify the inertia effects during the RCP. The simulation is based on the discrete element method, often used for rocks or soils modelling (Wang and Yan, 2011). It reveals to be an interesting way to model the mechanical behavior of brittle materials. It allows large displacements and strain and offers an alternative to the FEM by allowing a natural propagation of the crack (Hedjazi et al., 2012).

In this work, the DEM is used to simulate the dynamic fracture but only as a generation phase simulation, where the crack propagates manually (Nishioka, 1997)

The generation phase simulation was validated in FEM for the dynamic propagation of crack in plate structures (Kobayashi et al., 1976; Yagawa et al., 1977) or more recently in pipe structures (Kopp et al., 2014a). These models made possible to estimate the dynamic energy released rate by dissociating the structural (i.e kinetic energy) response and the materiel effect. Following, the review of the dynamic fracture in FEM (Nishioka, 1997), a gradual nodal relaxation was implemented in the DEM in order to evaluate the dynamic correction factor for RCP in HSS.

Final result of this work is an estimation of the critical energy released rate of the material.

2. Quasi-static and dynamic compression tests

2.1. Material

Hollow spheres are manufactured and patented (Blottiere et al., 1994) by ATECA SAS. The figure 1 presents an assembly of such hollow spheres with a average diameter D of 30 mm. They are composed of an epoxy resin with mineral powder to mainly prevent the spheres from sticking together during the manufacture process. Powder aggregates are in high proportion in the matrix. The grain size varies from 10 µm to 100 µm as it can be observed with the help of microscope observations; see figure 1(c).

The thickness ratio is defined by $R_t = e/r_m$, where e is the shell thickness and r_m the average radius ($r_m = (r_{in} + r_{ext})/2$), in figure 1(b). Tested hollow spheres present a diameter of $D_extt = 29.7 \pm 0.1$ mm, a radius ratio $R_t = 0.08$, and a mass $m = 6.30 \pm 0.5$ g. Two radius ratio are presented $R_t = 0.08$ and $R_t = 0.043$).

2.2. Methods

Uniaxial compressive tests on these hollow spheres were conducted on two machines: one classical compression machine (Zwick Roell Z250) for quasi-static tests and an original fly wheel (figure 2) for dynamic tests (Froustey et al., 2007; Viot, 2009). The rotational movement of the wheel is transformed into a translational movement. The velocity of the moving plates can be considered as constant due to the high amount of inertia of the wheel. Force sensors of 10 kN were used for both tests. A high speed camera (Photron SA-5) is used to capture the hollow sphere crushing, the propagation of cracks and the localization of its tip as shown in figure 3. 75000 frames per second with a resolution of 320 264 pixels is set.

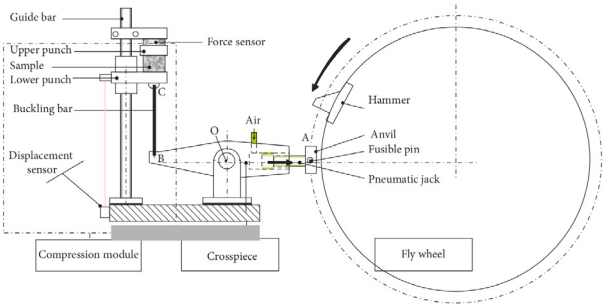

Fig. 2. The Fly wheel device for dynamic compression test (Viot, 2009).

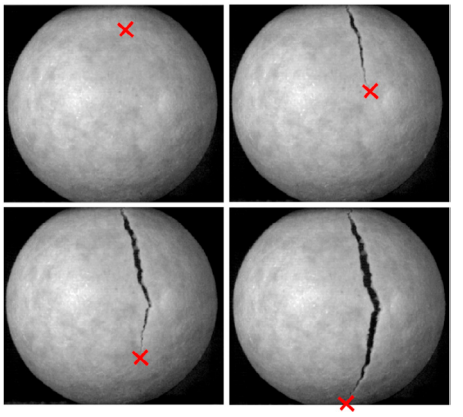

Fig. 3. Localization of the crack tip position thanks to a high speed camera (crack tip is marked with the red cross).

3. Discrete Element Simulation

3.1. Numerical details

As introduced in the first section of this paper, discrete elements can interact only by contact or can be connected by cohesive links like springs or 3D beams. As established in (André et al., 2012), DEM models using cohesive beams to link discrete elements are appropriate to model continuous material (Fillot et al., 2007; Jebahi et al., 2013; Coré et al., 2017). All of the deformation modes of the beam are taken into account: traction, compression, bending and torsion. The analytical model of the Euler-Bernoulli beam is used to compute the force and torques reactions acting on two discrete elements linked by a beam.

To position these cohesive links in the volume, a random compact packing of discrete elements is first generated. A beam network is assigned using a delaunay triangulation creating thus a random lattice. In this paper the DEM is only used as a lattice approach while offering the possibility in the future to model the contacts between the elements for more predictive simulation by taking into account non linear effects such as friction between the crack lips.

In order to create representative hollow sphere with discrete elements, a convergence analysis of the elastic phase was performed. A minimum number of discrete elements through the thickness are required to simulate continuous material depending on the geometry.

For thin structures like hollow spheres, a great number of elements are needed to keep enough elements in the thickness. The computing time to create this geometry (with a thickness ratio $R_t = 0.35$) varies from 4 seconds for 1 element in the thickness to 2600 seconds for 4.2 elements in the thickness. For the considered geometry of hollow sphere ($R_t = 0.08$ and $R_t = 0.043$), the computing time is much more important. It is then not reasonable to have more than 2 or 3 elements in the thickness. The cardinal number of the compact packing is approximately equal to 5.7 (the optimal value is 6.2 for isotropic representation) for the hollow sphere structure and is hardly influenced by the number of discrete elements through the thickness.

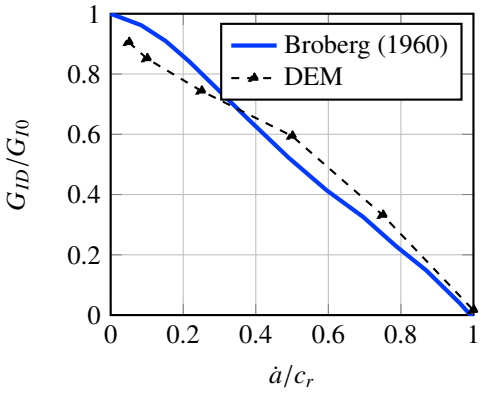

Fig. 4. Comparison between analytic and numeric solution of the dynamic correction ratio for a crack propagation in an infinite plate.

Despite this low value of coordination number, a value of two elements in the thickness has been retained to model the hollow sphere structure. A validation simulation comparing with the analytic solution for a circular plate submitted to central force gives an accuracy error less than 10% for a two element in the thickness model.

It is thus supposed to be a good compromise for calculation cost with a reasonnable accuracy of the behavior in the thickness.

3.2. Validation in dynamic propagation

To validate the crack tip opening methods, numerical results are compared to analytical ones. It has been shown that the higher the crack tip velocity is, the less the energy release rate is. In a crack propagation in a semi-infinite plate in mode I, the critical dynamic energy release rate decreases quasi-linearly (with the increase of the crack tip velocity between 0 c_r and 1 c_r with c_r the Rayleigh wave speed of the material) (Broberg, 1960). The figure 4 presents the results in term of the dynamic correction ratio (G_{ID}/G_{I0}), analytical and DEM results are compared. The dynamic energy release rate G_{ID} represents the energy released to the material during the propagation (Kopp et al., 2014b). The quasi-static energy release rate G_{I0} is computed considering that an increase in crack length Δa corresponds to an elastic unloading of a zone ahead of the crack tip of equivalent length Δa.

Results of these simulation shows a good concordance and validates our DEM implementation of a crack tip opening method.

4. Results and Discussions

Force and displacement measures for static and dynamic compression tests give two tendancies showed in figure 5. As expected, peak force is higher in dynamic (around 1 kN) than in static loading (around 800 N). The high dispersion of the results mainly comes from the process which gives approximate external and internal diameters.

Following this experimental result, the figure 6 shows the simulated crack opening of a HSS. The displacement magnitude field is plotted. For this simulation a first pre-stressed loading in compression is performed, giving an initial strain energy to the system. All energies are then recorded during the artificial propagation and the enrgy release rate is evaluated by assuming a perfect flat crack surface. The simulation is performed for different crack velocity regarding the Rayleigh wave speed C_r. The figure 7 presents the dynamic correction ratio for the critical energy release rate when a RCP occurs in a HSS for thickness ratios : 0.08 and 0.043 that corresponds to the ratio thickness of the HSS used in the exeperimental part.

In the same way that in pipes under pressure (Kopp et al., 2014a), the correction ratio decreases dramatically with the crack velocity reaching 0.1 for a crack velocity of $0.1C_r$ and a ratio thickness of 0.043. This ratio has a major influence of the inertial effects with a ratio of 2 between $r_t = 0.043$ and $r/t = 0.08$.

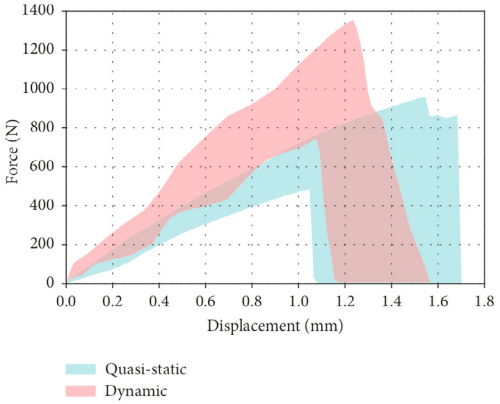

Fig. 5. Force-displacement curves for static and dynamic loadings (each results has been taken into account and gives the thickness of the red an blue curves).

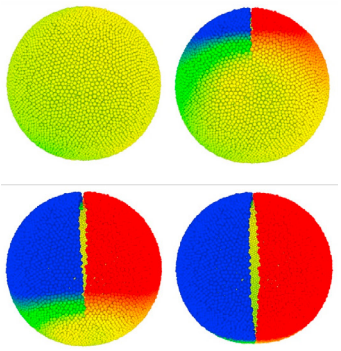

Fig. 6. Generation phase simulation for the crack opening in the HSS (plotted field is the magnitude displacement).

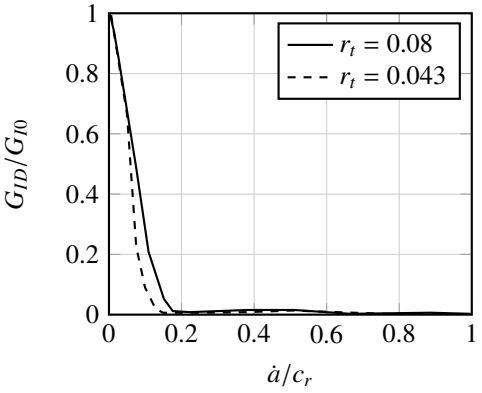

Fig. 7. Dynamic correction ratio for HSS regarding the crack velocity and the thickness.

This dynamic correction ratio is applied for the differents compression tests. the release rate G_{I0} is calculated by integrating the force-diplacement curve and by dividing the crack surface experimentally measured, following the formalism of Linear Elastic Fracture Mechanics. Results are given in the table 7. A high dispersion is observed for the G_{Idc} (from 0.4 to 0.84 kJ m^{-2}) where a unique value is attended. Nevertheless, similar values can be found in the litterature for similar materials : between 220 and 800 kJ m^{-2} for (Joudon, 2014), and between 100 and 1400 kJ m^{-2} for (Koh et al., 1993; Ragosta et al., 2005), where the same dispersion on the results is observed.

Table 1. Results synthesis for two thickness ratio and the static and dynamic tests, evaluation of the dynamic critical energy release rate G_{Idc}.

Sphere	r_t	v (m.s^{-1})	$\dot{a}/c_r$ (N)	G_{I0} (kJ/m^2)	G_{Idc} (kJ/m^2)
A	0.043	8.3 10^{-5}	0.08 ± 0.01	2.7 ± 0.4	0.45 ± 0.4
B	0.08	8.3 10^{-5}	0.12 ± 0.02	4.0 ± 0.7	0.84 ± 0.5
A	0.043	1.53 ± 0.17	0.09 ± 0.0	3.9 ± 1.2	0.69 ± 0.3
B	0.08	1.32 ± 0.18	0.14 ± 0.02	3.4 ± 0.3	0.4 ± 0.3

5. Conclusions

The dynamic fracture on a polymer material was investigated through a compression test on hollow sphere structures. The rapid crack propagation involves to take into account the inertia effects for the estimation of the critical energy release rate, which was done thanks to a dedicated DEM simulation. It appears that the HSS induces a non-neglectable inertia effect that needs to be evaluate for fracture test. The high dispersion of results shows that the crack velocity which has a significant infuence on the dynamic correction ratio and the crack surface need to be measured as accurate as possible.

References

André, D., Iordanoff, I., Charles, J.l., Néauport, J., 2012. Discrete element method to simulate continuous material by using the cohesive beam model. Computer Methods in Applied Mechanics and Engineering 213, 113–125.

Augustin, C., 2009. Multifunctional metallic hollow sphere structures: manufacturing, properties and application. Springer Science & Business Media.

Blottiere, Y., Chapuis, P., Valaud, M., 1994. Hollow spheres manufactured in synthetic materials, manufacturing process and application. URL: http://www.google.com/patents/EP0438352B1?cl=en. eP Patent 0,438,352.

Broberg, K.B., 1960. The propagation of a brittle crack. Arkiv Fysik 18, 159–192.

Coré, A., Kopp, J.B., Viot, P., Charles, J.L., Dau, F., 2017. Experimental Investigation and Discrete Element Modelling of Composite Hollow Spheres Subjected to Dynamic Fracture. International Journal of Polymer Science 2017, 1–15. URL: https://www.hindawi.com/journals/ijps/2017/7638482/, doi:10.1155/2017/7638482.

Fiedler, T., Solórzano, E., Öchsner, A., 2008. Numerical and experimental analysis of the thermal conductivity of metallic hollow sphere structures. Materials Letters 62, 1204–1207.

Fillot, N., Iordanoff, I., Berthier, Y., 2007. Modelling third body flows with a discrete element methoda tool for understanding wear with adhesive particles. Tribology International 40, 973–981.

Froustey, C., Lambert, M., Charles, J.L., Lataillade, J.L., 2007. Design of an Impact Loading Machine Based on a Flywheel Device: Application to the Fatigue Resistance of the High Rate Pre-straining Sensitivity of Aluminium Alloys. Experimental Mechanics 47, 709–721. URL: http://link.springer.com/10.1007/s11340-007-9082-4, doi:10.1007/s11340-007-9082-4.

Gasser, S., Paun, F., Cayzeele, A., Bréchet, Y., 2003. Uniaxial tensile elastic properties of a regular stacking of brazed hollow spheres. Scripta Materialia 48, 1617–1623.

Hedjazi, L., Martin, C., Guessasma, S., Della Valle, G., Dendievel, R., 2012. Application of the discrete element method to crack propagation and crack branching in a vitreous dense biopolymer material. International Journal of Solids and Structures 49, 1893–1899.

Jebahi, M., André, D., Dau, F., Charles, J.L., Iordanoff, I., 2013. Simulation of vickers indentation of silica glass. Journal of Non-Crystalline Solids 378, 15–24.

Joudon, V., 2014. Caractérisation exprimentale de l'initiation et de la propagation de fissure dans une résine époxy sous chargement dynamique. Thèse. Université de Valencienne et du Hainaut-Cambresis.

Kausch, H.H., 2012. Polymer fracture. volume 2. Springer Science & Business Media.

Kobayashi, A., Emery, A.F., Mall, S., 1976. Dynamic-finite-element and dynamic-photoelastic analyses of two fracturing homalite-100 plates. Experimental Mechanics 16, 321–328.

Koh, S.W., Kim, J.K., Mai, Y.W., 1993. Fracture toughness and failure mechanisms in silica-filled epoxy resin composites: effects of temperature and loading rate. Polymer 34, 3446–3455.

Kopp, J.B., Lin, J., Schmittbuhl, J., Fond, C., 2014a. Longitudinal dynamic fracture of polymer pipes. European Journal of Environmental and Civil Engineering 18, 1097–1105.

Kopp, J.B., Schmittbuhl, J., Noel, O., Lin, J., Fond, C., 2014b. Fluctuations of the dynamic fracture energy values related to the amount of created fracture surface. Engineering Fracture Mechanics 126, 178–189.

Nishioka, T., 1997. Computational dynamic fracture mechanics. International Journal of Fracture 86, 127–159.

Ragosta, G., Abbate, M., Musto, P., Scarinzi, G., Mascia, L., 2005. Epoxy-silica particulate nanocomposites: chemical interactions, reinforcement and fracture toughness. Polymer 46, 10506–10516.

Rahmé, P., Bouvet, C., Rivallant, S., Fascio, V., Valembois, G., 2012. Experimental investigation of impact on composite laminates with protective layers. Composites Science and Technology 72, 182–189.

Viot, P., 2009. Hydrostatic compression on polypropylene foam. International Journal of Impact Engineering 36, 975–989.

Wang, J., Yan, H., 2011. 3d dem simulation of crushable granular soils under plane strain compression condition. Procedia Engineering 14, 1713–1720.

Yagawa, G., Sakai, Y., Ando, Y., 1977. Analysis of a rapidly propagating crack using finite elements, in: Fast Fracture and Crack Arrest. ASTM International.

Yamini, S., Young, R.J., 1980. The mechanical properties of epoxy resins. Journal of materials science 15, 1823–1831.